Dynamical initialization of hydrodynamics for heavy-ion collisions at Beam Energy Scan energies

Lipei Du

Department of Physics, The Ohio State University, USA

with D. Everett and U. Heinz

Initial Stages 2021

January 13, 2021

IS2021
The VI[th] International Conference on the INITIAL STAGES OF HIGH-ENERGY NUCLEAR COLLISIONS

The Ohio State University

Motivation

Illustration of heavy-ion collisions

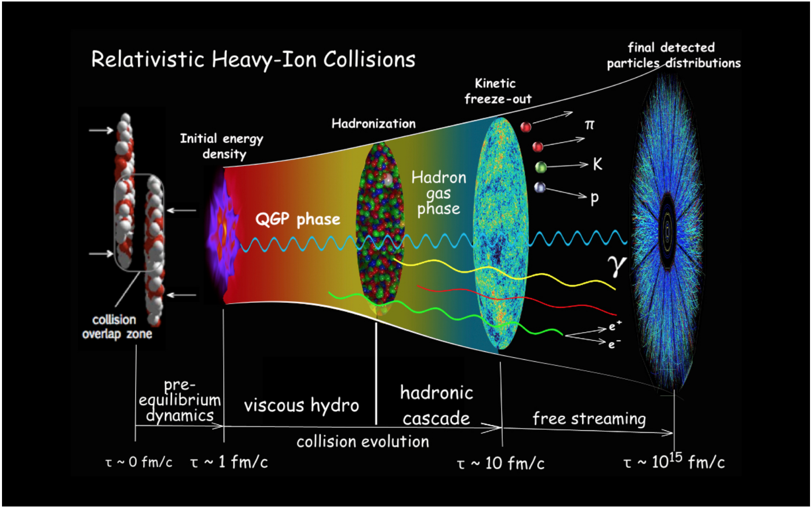

credit: Chun Shen

Exploring the QCD phase diagram with heavy-ion collisions

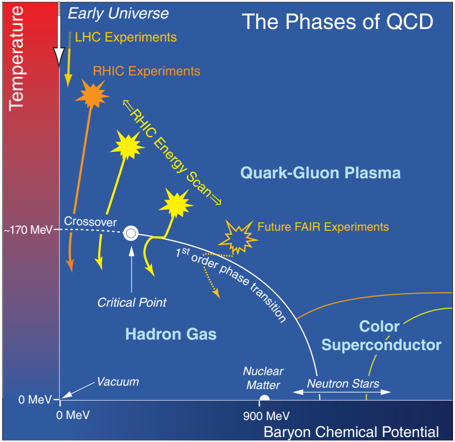

2007 NSAC Long Range Plan

Theoretical modeling of heavy-ion collisions at low energies:

- complicated interpenetration dynamics;
- dynamics of conserved charges;
- singularity associated with the QCD critical point in the thermal properties of the medium;
- large fluctuations and strong correlations near the critical point;
- ...

Dynamical initialization

Collision geometry

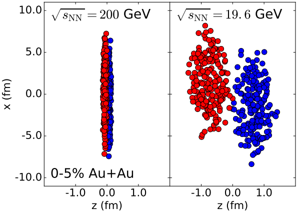

Collision geometry and overlap time of Au-Au collision [C. Shen and B. Schenke, 1710.00881, Du et al. 1807.04721].

Collision geometry

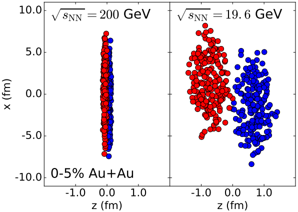

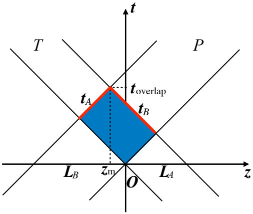

Collision geometry and overlap time of Au-Au collision [C. Shen and B. Schenke, 1710.00881, Du et al. 1807.04721].

Collision geometry

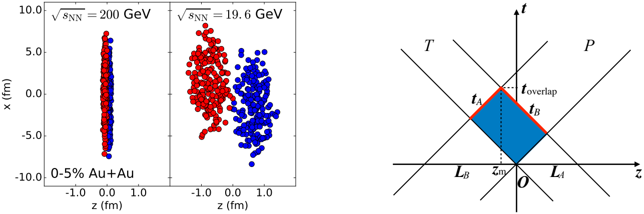

Collision geometry and overlap time of Au-Au collision [C. Shen and B. Schenke, 1710.00881, Du et al. 1807.04721].

- At low collision energies (e.g. Beam Energy Scan energies), the space-time history of nuclear interpenetration is complicated;
- Hybrid descriptions of heavy-ion collision involving hydrodynamics require (3+1)D initial conditions in these cases;

Collision geometry

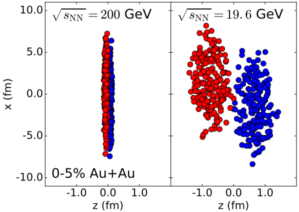

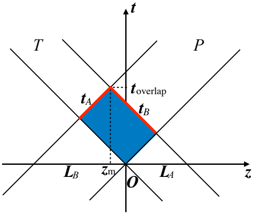

Collision geometry and overlap time of Au-Au collision [C. Shen and B. Schenke, 1710.00881, Du et al. 1807.04721].

- At low collision energies (e.g. Beam Energy Scan energies), the space-time history of nuclear interpenetration is complicated;
- Hybrid descriptions of heavy-ion collision involving hydrodynamics require (3+1)D initial conditions in these cases;
- Two main ingredients needed:
  - energy deposition and charge doping in space-time, e.g., hadron-string transport approaches;
  - criterion of switching to hydrodynamics from point to point (hydrodynamization/fluidization);

Construction of (3+1)D initial conditions

- Some dynamical initialization models for hydrodynamics at low beam energies

References	Dynamics	Smearing kernel	Hydro
Shen et al.,	MC-Glauber + string	Gaussian with $\sigma_\perp$ and σ_η	(3+1)D MUSIC
Du et al.,	Modified UrQMD	Lorentz invariant kernel	(3+1)D BESHYDRO
Naboka et al.,	Relaxation model of $T^{\mu\nu}$	Gaussian with R_x and R_y	(2+1)D vHLLE
Akamatsu et al.,	JAM	Lorentz invariant kernel	HLLE algorithm
Okai et al., & Kanakubo et al.,	PYTHIA	Gaussian with $\sigma_\perp$ and σ_η	Y. Tachibana

Construction of (3+1)D initial conditions

- Some dynamical initialization models for hydrodynamics at low beam energies

References	Dynamics	Smearing kernel	Hydro
Shen et al.,	MC-Glauber + string	Gaussian with $\sigma_\perp$ and σ_η	(3+1)D MUSIC
Du et al.,	Modified UrQMD	Lorentz invariant kernel	(3+1)D BESHYDRO
Naboka et al.,	Relaxation model of $T^{\mu\nu}$	Gaussian with R_x and R_y	(2+1)D vHLLE
Akamatsu et al.,	JAM	Lorentz invariant kernel	HLLE algorithm
Okai et al., & Kanakubo et al.,	PYTHIA	Gaussian with $\sigma_\perp$ and σ_η	Y. Tachibana

- Comparison between initial conditions based on transport model (modified-UrQMD) [L. Du et al., 1807.04721] and dynamical string model [C. Shen and B. Schenke, 1710.00881] (see also Chun Shen's talk, Wed. 19:25, Session CD)

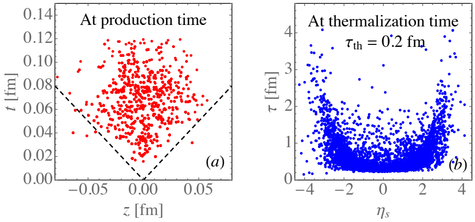

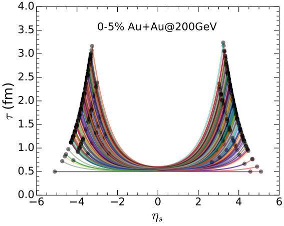

Violation of boost-invariance

- At BES energies, initial energy deposition and baryon doping in modified-UrQMD are not boost-invariant:

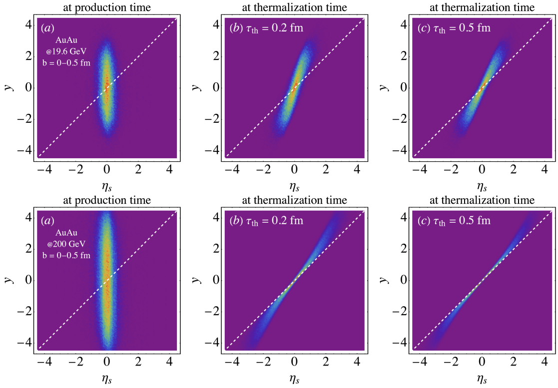

Space-time rapidity and rapidity distributions of produced particles.

- Initial distribution evolves towards boost-invariance by longitudinal free-streaming;
- This evolution is faster at higher collision energies.

Violation of boost-invariance

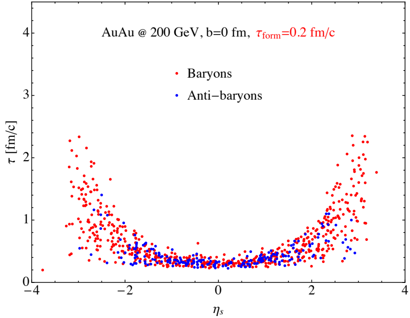

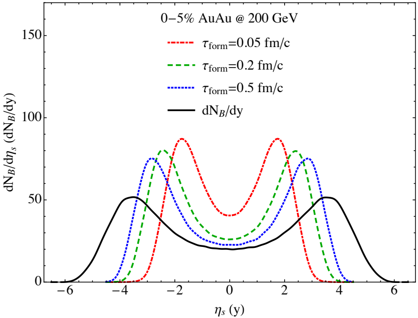

Space-time rapidity and rapidity distributions of baryons, anti-baryons and net baryons [L. Du et al., 1807.04721] (note: τ_{form} is the thermalization time).

- The initial space-time distribution have large uncertainties (within our model from the value of the thermalization time).
- Similar rapidity distributions can correspond to very different space-time rapidity distributions, and different space-time rapidity distributions may lead to different hydrodynamic evolution.

Dynamical sources: formalism

- Hydrodynamics with dynamical sources (d_μ being covariant derivative):

$$\begin{aligned} d_\mu T^{\mu\nu}_{\mathrm{fluid}}(x) &= \mathcal{J}^\nu_{\mathrm{source}}(x) \equiv -d_\mu T^{\mu\nu}_{\mathrm{p}}(x)\ , \\ d_\mu N^{\mu}_{\mathrm{fluid}}(x) &= \rho_{\mathrm{source}}(x) \equiv -d_\mu N^{\mu}_{\mathrm{p}}(x)\ . \end{aligned}$$

Dynamical sources: formalism

- Hydrodynamics with dynamical sources (d_μ being covariant derivative):

$$\begin{aligned} d_\mu T^{\mu\nu}_{\text{fluid}}(x) &= \mathcal{J}^\nu_{\text{source}}(x) \equiv -d_\mu T^{\mu\nu}_{\text{p}}(x) , \\ d_\mu N^{\mu}_{\text{fluid}}(x) &= \rho_{\text{source}}(x) \equiv -d_\mu N^{\mu}_{\text{p}}(x) . \end{aligned}$$

- Energy-momentum tensor and baryon current of the particles are given by [D. Oliinychenko and H. Petersen, Phys.Rev. C93 (2016) 034905]

$$\begin{aligned} T^{\mu\nu}_{\text{p}}(t, \boldsymbol{r}) &= \sum_i \frac{p_i^\mu p_i^\nu}{p_i^0} K(\boldsymbol{r} - \boldsymbol{r}_i(t),\ p_i)\Phi(t - t_{\text{th},i}) , \\ N^{\mu}_{\text{p}}(t, \boldsymbol{r}) &= \sum_i b_i \frac{p_i^\mu}{p_i^0} K(\boldsymbol{r} - \boldsymbol{r}_i(t),\ p_i)\Phi(t - t_{\text{th},i}) . \end{aligned}$$

Dynamical sources: formalism

- Hydrodynamics with dynamical sources (d_μ being covariant derivative):

$$
\begin{aligned}
d_\mu T^{\mu\nu}_{\mathrm{fluid}}(x) &= \mathcal{J}^\nu_{\mathrm{source}}(x) \equiv -d_\mu T^{\mu\nu}_{\mathrm{p}}(x) \,, \\
d_\mu N^{\mu}_{\mathrm{fluid}}(x) &= \rho_{\mathrm{source}}(x) \equiv -d_\mu N^{\mu}_{\mathrm{p}}(x) \,.
\end{aligned}
$$

- Energy-momentum tensor and baryon current of the particles are given by [D. Oliinychenko and H. Petersen, Phys.Rev. C93 (2016) 034905]

$$
\begin{aligned}
T^{\mu\nu}_{\mathrm{p}}(t,\boldsymbol{r}) &= \sum_i \frac{p_i^\mu p_i^\nu}{p_i^0} K(\boldsymbol{r}-\boldsymbol{r}_i(t),\, p_i)\Phi(t-t_{\mathrm{th},i}) \,, \\
N^{\mu}_{\mathrm{p}}(t,\boldsymbol{r}) &= \sum_i b_i \frac{p_i^\mu}{p_i^0} K(\boldsymbol{r}-\boldsymbol{r}_i(t),\, p_i)\Phi(t-t_{\mathrm{th},i}) \,.
\end{aligned}
$$

- The spatial smearing kernel in the particles' rest frame and lab frame is given by

$$
\begin{aligned}
K_i(t_{\mathrm{rf}}, \boldsymbol{x}_{\mathrm{rf}}, p_i) &= \frac{1}{(2\pi\sigma^2)^{3/2}} \exp\left[\frac{-(\boldsymbol{x}_{\mathrm{rf}}-\boldsymbol{r}_{\mathrm{rf},i})^2}{2\sigma^2}\right] , \\
K_i(x) &= \frac{\gamma_i}{(2\pi\sigma^2)^{3/2}} \exp\left[-\frac{\Delta\boldsymbol{r}^2 + (\Delta\boldsymbol{r}\cdot\boldsymbol{u}_i)^2}{2\sigma^2}\right] ,
\end{aligned}
$$

where $\Delta\boldsymbol{r} = \boldsymbol{r} - \boldsymbol{r}_i(t_{\mathrm{th},i})$, $\boldsymbol{u}_i = \gamma_i \boldsymbol{\beta}_i$.

Dynamical sources: smearing kernel

- The sources and tensors are constructed in Cartesian coordinates and then mapped to Milne coordinates:

$$t(\tau, \eta_s) = \tau \cosh \eta_s \ , \quad z(\tau, \eta_s) = \tau \sinh \eta_s \ .$$

Dynamical sources: smearing kernel

- The sources and tensors are constructed in Cartesian coordinates and then mapped to Milne coordinates:

$$t(\tau, \eta_s) = \tau \cosh \eta_s \ , \quad z(\tau, \eta_s) = \tau \sinh \eta_s \ .$$

- 3D initial condition from AMPT model [L. Pang, Q. Wang and X.-N. Wang, 1205.5019]

$$T^{\mu\nu}(\tau_0, x, y, \eta_s) = K \sum_i \frac{p_i^\mu p_i^\nu}{p_i^\tau} \frac{1}{\tau_0 \sqrt{2\pi\sigma_{\eta_s}^2}} \frac{1}{2\pi\sigma_r^2} \exp\left[-\frac{(x-x_i)^2 + (y-y_i)^2}{2\sigma_r^2} - \frac{(\eta_s - \eta_{is})^2}{2\sigma_{\eta_s}^2} \right],$$

Dynamical sources: smearing kernel

- The sources and tensors are constructed in Cartesian coordinates and then mapped to Milne coordinates:

$$t(\tau, \eta_s) = \tau \cosh \eta_s \ , \quad z(\tau, \eta_s) = \tau \sinh \eta_s \ .$$

- 3D initial condition from AMPT model [L. Pang, Q. Wang and X.-N. Wang, 1205.5019]

$$T^{\mu\nu}(\tau_0, x, y, \eta_s) = K \sum_i \frac{p_i^\mu p_i^\nu}{p_i^\tau} \frac{1}{\tau_0 \sqrt{2\pi\sigma_{\eta_s}^2}} \frac{1}{2\pi\sigma_r^2} \exp\left[-\frac{(x-x_i)^2+(y-y_i)^2}{2\sigma_r^2} - \frac{(\eta_s-\eta_{is})^2}{2\sigma_{\eta_s}^2}\right],$$

- Dynamical string model [C. Shen and B. Schenke, 1710.00881]

$$f_{\rm smear}(x^\alpha; x_i^\alpha) = \frac{\delta(\tau-\tau_i)}{\tau} f_\perp(x, y; x_i, y_i) f_{\eta_s}(\eta_s; \eta_{s,i}).$$

with Gaussian smearing profiles in the transverse and longitudinal directions,

$$f_\perp(x, y; x_i, y_i) = \frac{1}{\pi\sigma_\perp^2} \exp\left[-\frac{(x-x_i)^2-(y-y_i)^2}{\sigma_\perp^2}\right],$$

$$f_{\eta_s}(\eta_s; \eta_{s,i}) = \frac{1}{\sqrt{\pi}\sigma_{\eta_s}} \exp\left[-\frac{(\eta_s-\eta_{s,i})^2}{\sigma_{\eta_s}^2}\right].$$

Dynamical sources: smearing kernel

- Mapping a Gaussian smearing kernel w.r.t $(t,\ z)$ and $(\tau,\ \eta_s)$ in different coordinate systems

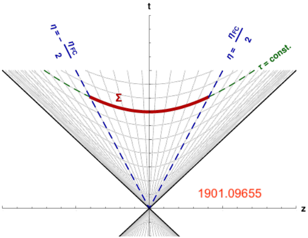

Dynamical sources: smearing kernel

- Mapping a Gaussian smearing kernel w.r.t $(t,\ z)$ and $(\tau,\ \eta_s)$ in different coordinate systems

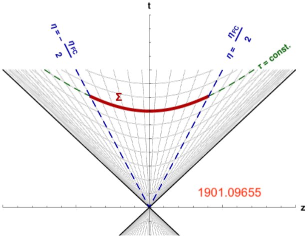

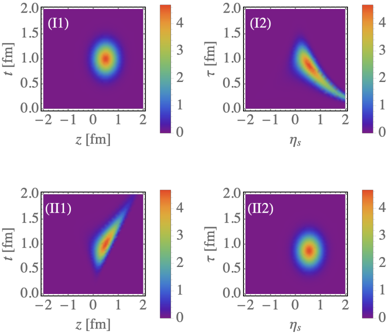

Map of a Gaussian kernel between Cartesian and Milne coordinates

Dynamical sources: smearing kernel

- Mapping a Gaussian smearing kernel w.r.t $(t,\ z)$ and $(\tau,\ \eta_s)$ in different coordinate systems

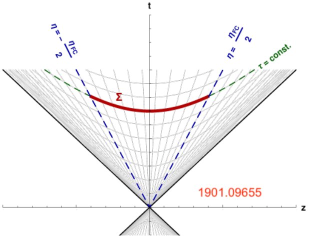

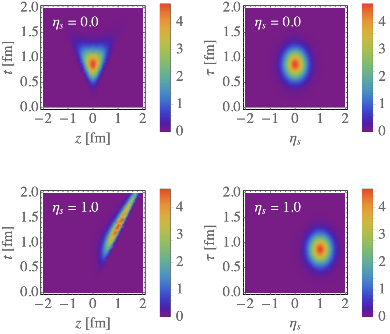

Map of a Gaussian kernel between Cartesian and Milne coordinates (at $\eta_s = 0$ and 1.)

Dynamical sources: smearing kernel

- Mapping a Gaussian smearing kernel w.r.t $(t,\ z)$ and $(\tau,\ \eta_s)$ in different coordinate systems

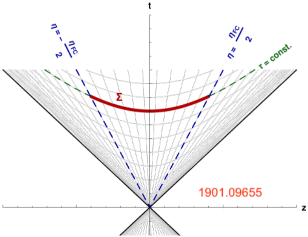

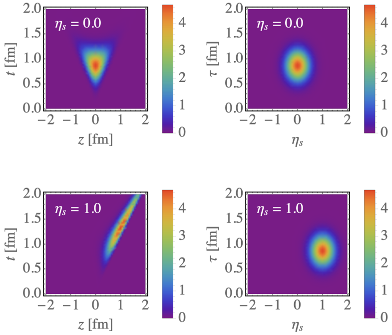

Map of a Gaussian kernel between Cartesian and Milne coordinates (at $\eta_s = 0$ and 1.)

- For construction of (3+1)D initial conditions at low beam energies, more attention should be paid on the smearing kernel.

Dynamical sources: Lorentz contraction and time dilation

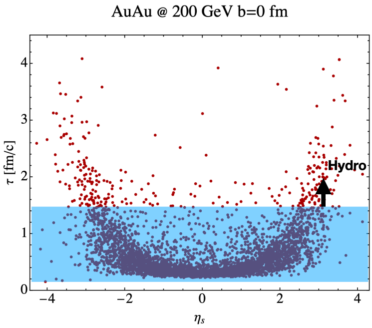

Dynamical sources: Lorentz contraction and time dilation

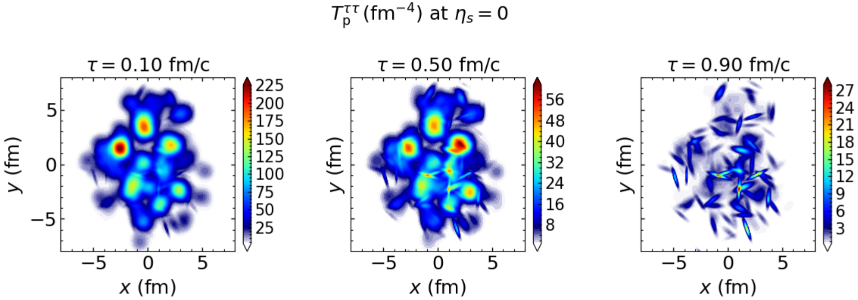

$T^{\tau\tau}$ of the particles at mid-rapidity (Au-Au 200 GeV, $b = 5.0$–5.5 fm).

Dynamical sources: Lorentz contraction and time dilation

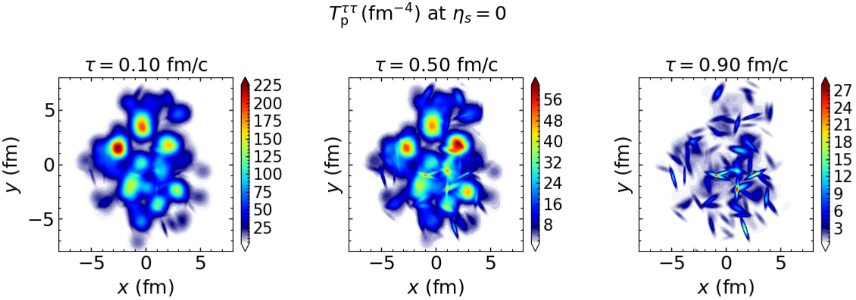

$T^{\tau\tau}$ of the particles at mid-rapidity (Au-Au 200 GeV, $b = 5.0$–5.5 fm).

- Assuming the same free-streaming time in particles' rest frame, particles with higher velocity will propagate to larger τ and η_s;
- with larger Lorentz contraction, these particles introduce larger anisotropy at later times and at larger space-time rapidity.

Gaussian width of the smearing kernel

- Evolution in initial conditions and effects from different smearing width (at $\eta_s = 1.5$)

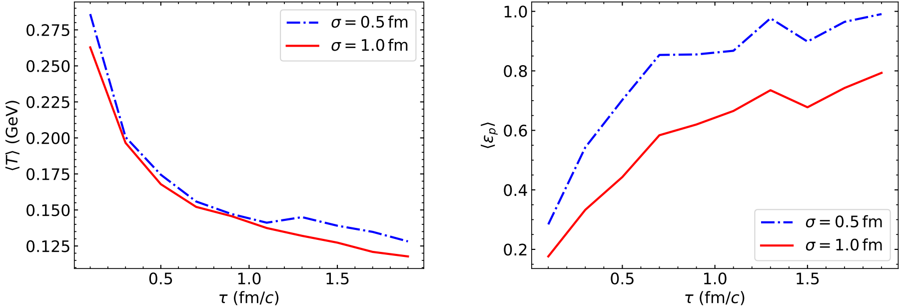

Evolution of the averaged temperature (left) and transverse momentum anisotropy (right) at $\eta_s = 1.5$ with $\tau_{\rm th} = 0.2$ fm/c and Gaussian smearing width σ =0.5 and 1.0 fm in Cartesian coordinates (Au-Au 200 GeV, $b = 5.0$-5.5 fm).

- Averaged temperature and transverse momentum anisotropy

$$\langle T\rangle = \frac{\int dxdy\ e(x,y)T(x,y)}{\int dxdy\ e(x,y)}, \quad \langle \epsilon_p\rangle = \sqrt{\frac{\langle T^{xx}-T^{yy}\rangle^2 + \langle 2T^{xy}\rangle^2}{\langle T^{xx}+T^{yy}\rangle^2}}$$

Different smearing kernels

- Evolution in initial conditions with different smearing kernel (at $\eta_s = 1.5$)

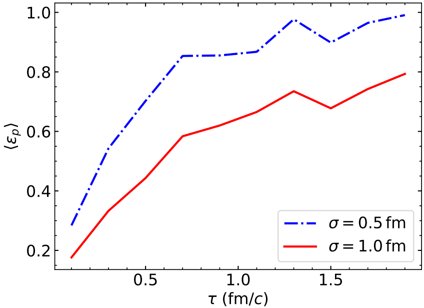

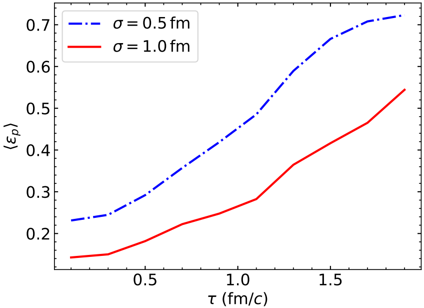

Comparison of transverse momentum anisotropy at $\eta_s = 1.5$ with a smearing kernel in Cartesian (left) and Milne (right) coordinates.

- Smearing kernel with Lorentz contraction in Cartesian coordinates results in larger anisotropy and more fluctuations.

Perspectives on transport coefficients extraction

- To extract transport properties (such as charge diffusion constants) of fireballs created at low beam energies, we need a well-constrained (3+1)D initial condition [C. Shen, G. Denicol, C. Gale, S. Jeon, A. Monnai, B. Schenke, 1704.04109; C. Shen and B. Schenke, 1710.00881; G. Denicol, C. Gale, S. Jeon, A. Monnai, B. Schenke, and C. Shen, 1804.10557; L. Du, U. Heinz, G. Vujanovic, 1807.04721].

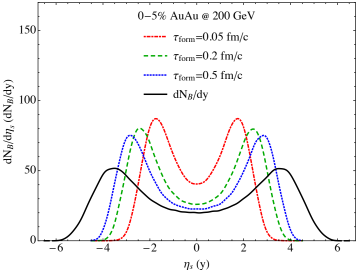

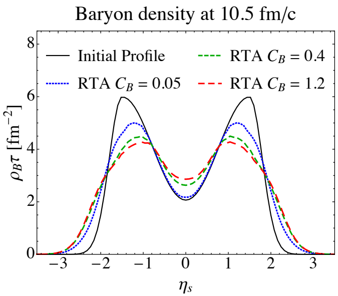

(left) initial baryon stopping; (right) hydrodynamic transport.

Perspectives on transport coefficients extraction

- To extract transport properties (such as charge diffusion constants) of fireballs created at low beam energies, we need a well-constrained (3+1)D initial condition [C. Shen, G. Denicol, C. Gale, S. Jeon, A. Monnai, B. Schenke, 1704.04109; C. Shen and B. Schenke, 1710.00881; G. Denicol, C. Gale, S. Jeon, A. Monnai, B. Schenke, and C. Shen, 1804.10557; L. Du, U. Heinz, G. Vujanovic, 1807.04721].

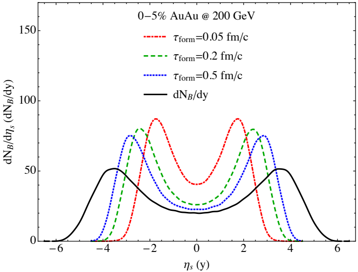

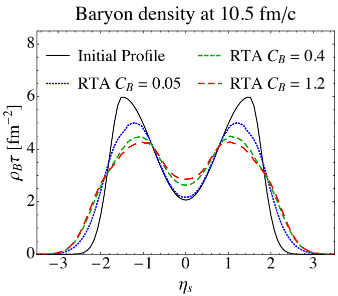

(left) initial baryon stopping; (right) hydrodynamic transport.

- To disentangle effects from initial baryon stopping and hydrodynamic transport;
- It's useful to have both distributions in space-time rapidity and rapidity in the initial stage, since initial conditions are mostly in space-time rapidity whereas observables are in (pseudo-)rapidity.

Perspectives on transport coefficients extraction

- Different smearing kernels may result in different event plane decorrelation and extraction of $\eta/s(\mu, T)$ at low beam energies.

Perspectives on transport coefficients extraction

- Different smearing kernels may result in different event plane decorrelation and extraction of $\eta/s(\mu, T)$ at low beam energies.
- Using rapidity differential anisotropic flow to constrain the temperature dependence of $\eta/s(T)$ [G. Denicol, A. Monnai, and B. Schenke, 1512.01538].

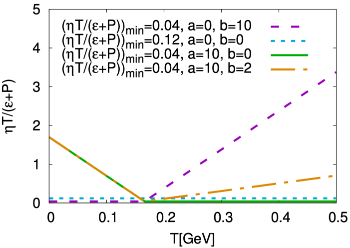

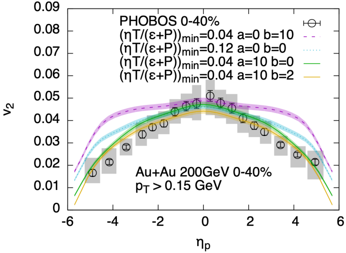

Note that within the current model, one expects larger isotropy at large space-time rapidity.

Summary

Summary

- At low beam energies, dynamical initialization of hydrodynamics with (3+1)-dimensional initial conditions becomes important.
- With violation of boost-invariance at low beam energies, different smearing kernels will be of phenomenological relevance: extraction of viscosity, event plane decorrelation, etc.
- More attention should be paid on possible effects from smearing kernels.

Thank you very much!